bjh research paper

Stimulation of invariant natural killer T cells by α-Galactosylceramide activates the JAK-STAT pathway in endothelial cells and reduces angiogenesis in the 5T33 multiple myeloma model

Haneen Nur,[1,2] Luigia Rao,[3] Maria Antonia Frassanito,[3] Hendrik De Raeve,[4] Domenico Ribatti,[5,6] Josué Kunjom Mfopou,[7] Els Van Valckenborgh,[1] Elke De Bruyne,[1] Angelo Vacca,[3] Karin Vanderkerken[1]* and Eline Menu[1]*

[1]Department of Haematology and Immunology, Myeloma Centre Brussels, Vrije Universiteit Brussel (VUB), Brussels, Belgium, [2]Department of Biology, Faculty of Science and Technology, Hebron University, Hebron, Palestine, [3]Department of Biomedical Sciences and Human Oncology, University of Bari "AldoMoro" Medical School, Bari, Italy, [4]Department of Surgical Pathology, Universitair Ziekenhuis Brussel, Brussels, Belgium, [5]Department of Basic Medical Sciences, Neurosciences and Sensory Organs, University of Bari Medical School, [6]National Cancer Institute "Giovanni Paolo II", Bari, Italy and [7]Cell Differentiation Unit, Diabetes Research Centre, Vrije Universiteit Brussel (VUB), Brussels, Belgium

Received 6 June 2014; accepted for publication 9 July 2014

Correspondence: Eline Menu, PhD, Haematology and Immunology laboratory, Myeloma Centre, Faculty of Medicine and Pharmacy, Vrije Universiteit Brussel, room D006, Laarbeeklaan 103, 1090 Jette, Belgium.
E-mail: Eline.Menu@vub.ac.be
*These authors contributed equally to this work.

Summary

Tumour pathogenesis in multiple myeloma (MM) correlates with a high vascular index. Therefore, targeting angiogenesis is an important therapeutic tool to reduce MM progression. This study aimed to investigate the role of invariant natural killer T (iNKT) cells in angiogenesis and the mechanisms behind the stimulation by α-Galactosylceramide (α-GalCer). We have previously found that α-GalCer could increase the survival of 5T33MM mice and here we demonstrate that α-GalCer reduces the microvessel density. We performed both *in vivo* and *in vitro* angiogenic assays to confirm this observation. We found that conditioned medium of α-GalCer stimulated iNKT cells reduced neovascularization in the chick chorioallantoic membrane and in matrigel plug assays. Moreover, we observed a reduction in proliferation, migration and network formation and an induction of apoptosis upon exposure of murine endothelial cell lines to this conditioned medium. We furthermore observed that the JAK-STAT signaling pathway was highly activated in endothelial cells in response to stimulated iNKT cells, indicating the possible role of IFN-γ in the anti-angiogenic process. In conclusion, these results highlight the possibility of recruiting iNKT cells to target MM and angiogenesis. This gives a rationale for combining immunotherapy with conventional anti-tumour treatments in view of increasing their therapeutic potential.

Keywords: multiple myeloma, invariant natural killer T cells, α-Galactosylceramide, MM-induced angiogenesis, JAK-STAT pathway.

Natural killer T (NKT) cells are a small population of T lymphocytes derived from the thymus at the double positive ($CD4^+CD8^+$) stage of T cell development (Nakagawa *et al*, 1997; Brennan *et al*, 2013). These cells are found both in mice and humans (Matsuda *et al*, 2008), and are defined by co-expression of markers of T cells and NK cells. NKT cells are classified into different subpopulations, of which the type I NKT cells are referred to as invariant NKT (iNKT) cells. iNKT cells use their unique canonical semi-invariant T cell receptor with the Vα14.Jα18 chain joined to Vβ8.2/β7/β2 in mice and Vα24.Jα18 joined to Vβ11 in humans to recognize self and foreign lipid antigens, presented by CD1d molecules of antigen presenting cells, such as dendritic cells (DCs) (Van Kaer, 2007; Vivier *et al*, 2012; Kumar & Delovitch, 2014). The discovery of α-Galactosylceramide (α-GalCer), a glycolipid marine-derived ligand for iNKT cells, made it possible to examine the anti-tumour activity of these cells (Van Kaer, 2005; Neparidze & Dhodapkar, 2009). In addition, as

First published online 21 August 2014
doi:10.1111/bjh.13092

iNKT cells can potently respond to α-GalCer by secreting copious amounts of cytokines, such as γ-interferon (IFN-γ) (Cerundolo *et al*, 2009), the development of iNKT immunotherapy as an applicable tool to fight cancer is under investigation. The role of iNKT cells in tumour suppression has been reported in different murine models and in several clinical trials (reviewed in (Nur *et al*, 2013a)). With regards to multiple myeloma (MM), a monoclonal B-cell malignancy caused by the accumulation of plasma cells in the bone marrow (BM), the role of iNKT cells has been described by several groups both clinically and preclinically (Dhodapkar *et al*, 2003; Spanoudakis *et al*, 2009; Mattarollo *et al*, 2012). We have previously demonstrated that α-GalCer administration on the same day of MM inoculation significantly increased the survival of 5T33MM diseased mice from 22 d (in non-treated mice) to 29 d (in treated mice) (Nur *et al*, 2013b). However, the mechanisms associated with MM regression are not fully understood.

It is now well known that angiogenesis is an important process required for tumour growth, survival and metastasis (Tandle *et al*, 2004) and is defined as the generation of new vasculature from pre-existing blood vessels. This phenomenon requires different steps, including endothelial cell (EC) proliferation, migration and new vascular plexus formation (Jakob *et al*, 2006; Vacca & Ribatti, 2006; Ria *et al*, 2011). MM-induced angiogenesis results from an unbalanced ratio between pro- and anti-angiogenic factors in the BM microenvironment, which is switched to favour the angiogenic path during MM progression (Hanahan & Folkman, 1996; Vacca *et al*, 2001; Bhutani *et al*, 2014). The increased MM-induced angiogenesis is correlated to poor prognosis (Giles, 2002; Moehler *et al*, 2004).

IFN-γ is implicated in tumour suppression, and one of the proposed anti-tumour mechanisms is the inhibition of tumour angiogenesis (Ikeda *et al*, 2002). Hayakawa *et al* (2002) reported that IFN-γ secreted by both α-GalCer- activated iNKT cells and NK cells can mediate inhibition of tumour angiogenesis in some murine solid tumours. However, the contribution of the immune cells as anti-angiogenic players in haematological malignancies is not clear and needs more investigation. Therefore, this study aimed to investigate the role of iNKT cells in inhibiting MM induced-angiogenesis *in vivo* in the 5T33MM model, and to examine the mechanisms behind this inhibition *in vitro*.

Materials and methods

Animals

C57BL/KaLwRij mice were purchased from Harlan CPB (Horst, the Netherlands) and were 6–8 weeks old when used. They were housed and treated following the guidelines of the Ethical Committee for Animal Experiments, VUB (license no. LA1230281). Approval for these specific experiments was obtained from the committee under the number 09-281-5. The animal ethics meet the standards required by the United Kingdom Coordinating Committee on Cancer Research Guidelines (UKCCCR, 1998).

5T33MM mouse model

The 5T33MM model originated spontaneously in elderly C57BL/KaLwRij mice as described previously (Radl *et al*, 1979; Vanderkerken *et al*, 2003) and have since been propagated by intravenous injection of the diseased BM into young syngeneic recipients, which usually develop MM in 3–4 weeks (Vanderkerken *et al*, 2005).

α-Galactosylceramide preparation

α-Galactosylceramide (α-GalCer), dissolved in dimethylsulphoxide at 1 mg/ml was kindly provided by Dr. S. Van Calenbergh (University of Ghent, Belgium) and kept at −20°C.

For *in vivo* use, α-GalCer was dissolved in phosphate-buffered saline (PBS; Lonza, Braine-l'Alleud, Belgium) at a concentration of 10 μg/ml. Then the solution was incubated at 80°C for 20 min followed by sonication for 10 min. For *in vitro* use, α-GalCer was dissolved in vehicle (96 mg/ml sucrose, 10 mg/ml sodium deoxycholate and 0·05% Tween 20) at a stock solution of 10 μg/ml, which was further diluted to 100 ng/ml as a final working concentration. The stock solution was incubated and sonicated as described above.

In vivo *injection of α-GalCer in 5T33MM mouse model*

5T33MM inoculated mice ($0{\cdot}5 \times 10^6$ cells) were treated with 2 μg α-GalCer or vehicle (200 μl PBS) at 4-d intervals, as previously described (Hayakawa *et al*, 2002). The i.p. injection was started on the inoculation day and terminated when the vehicle mice became sick. All animals were sacrificed; livers and spleens were removed and weighed. Blood samples were collected to determine serum paraprotein (M-protein) levels and BM samples were isolated to determine plasmacytosis (tumour load), which was assessed on May-Grünwald Giemsa stained cytosmears. To evaluate IFN-γ levels, serum was collected 18 h after α-GalCer administration at weekly intervals and analysed by ELISA according to the manufacturer's instructions (eBioscience, Vienna, Austria).

Measurement of BM angiogenesis

Blood vessel-CD31 immunohistochemistry was performed on zinc-fixed, paraffin-embedded BM sections as previously described (Van Valckenborgh *et al*, 2002; Menu *et al*, 2006). Briefly, the femur was fixed in zinc fixative for 48 h, decalcified for 48 h and embedded in paraffin. The sections were blocked with normal goat serum for 30 min, followed by overnight incubation with a rat anti-CD31 antibody

(PECAM-1, 1:10; BD Biosciences, Erembodegem, Belgium) at 4°C. A biotin-conjugated goat anti-rat specific polyclonal antibody (1:75; BD Biosciences) was used as secondary antibody. For visual detection, a streptavidin-horseradish peroxidase conjugate was used in combination with Tyramide Signal Amplification (TSA; NEN Life Science Products, Boston, MA, USA). Microvessel density (MVD) was determined by counting under the microscope (×200) the number of blood vessels per 0·22 mm^2 in the area with the highest vessel density (hot spot).

Isolation and purification of murine liver iNKT

Murine liver iNKT cells were isolated by liver perfusion as previously described (Nur *et al*, 2013b). Mice were anesthetized i.p. with a mixture of 75 mg/kg ketamine (CEVA Santé Animale, Machelen, Belgium) and 50 mg/kg medetomidine hydrochloride (Virbac, Leuven, Belgium), and the abdomen was opened immediately. Renal veins were tied and the inferior vena cava and portal veins were cannulated simultaneously with 18G needles. Livers were perfused with 25 ml of 10 mmol/l EDTA/PBS (pH 7·4) at 7 ml/min within a closed sterilised catheter system using a peristaltic pump (Gilson, Villiers, France). The outflow was collected, washed and lysed with 2 ml Red Blood Cell lysis buffer for 1 min and neutralized with 10% fetal calf serum (FCS; Biochrom AG, Berlin, Germany) in RPMI-1640 medium (Lonza) supplemented with 1% penicillin/streptomycin, L-glutamine, and MEM NEAA-pyruvate (Lonza) (RPMI-1640 supplemented medium) (Fang *et al*, 2010). Mononuclear cells from at least 6 liver perfusions were collected for purification through magnetic-activated cell sorting, using a mouse $NK1.1^+$ iNKT cell isolation kit according to the manufacturer's instructions (Miltenyi Biotec, Bergisch Gladbach, Germany). Purity of the liver iNKT cell preparation was about 90% as determined by flow cytometry (FACS Canto; BD Biosciences).

Preparation of conditioned media and controls

BM-derived DCs were prepared as described previously (Nur *et al*, 2013b). DCs were loaded overnight with 100 ng/ml α-GalCer or vehicle. Several conditioned media (CM) were prepared from DCs co-cultured with iNKT cells at 4:1 ratio in the presence (CM^{+Gal}) or absence (CM^{-Gal}) of α-GalCer, or from single cultures of iNKT cells alone (CM^{NKT}) and DCs alone (CM^{DC}). These cultures were performed in RPMI-1640 supplemented medium with 5% FCS and incubated at 37°C and 5% CO_2. The supernatant was harvested after 72 h and frozen at −20°C until use. The controls for the *in vitro* experiments were as follows: 5% FCS in RPMI-1640 supplemented medium (Control), 50 ng/ml mouse IFN-γ recombinant protein (eBioscience) (rIFN-γ) and 10 μg/ml anti-mouse IFN-γ Ab (clone XMG1.2, BioLegend, San diego, CA, USA) (CM^{+Gal} + α-IFN-γ).

Chick chorioallantoic membrane (CAM) assay

Fertilized white Leghorn chicken eggs were incubated in triplicate at 37°C at constant humidity. On day 3, the shell was opened and 2–3 ml of albumen was removed to detach the CAM. On day 8, the CAMs were implanted with 1 mm^3 sterilized gelatin sponges (Gelfoam, Upjohn®, Kalamazoo, MI, USA) loaded with control medium, CM^{+Gal}, CM^{-Gal}, CM^{NKT} or CM^{DC}. The angiogenic response in the CAM was evaluated on day 12 in three separate 50× fields as the number of vessels converging toward the sponge, and photographed *in ovo* (Olympus stereomicroscope, Rozzano, Italy).

Matrigel plug assay

Female non-obese diabetic severe combined immunodeficiency (NOD-*scid*) mice, 6–8 weeks of age, were anesthetized with tribromoethanol (Avertin; 0·5 ml i.p., Sigma-Aldrich, Diegem, Belgium) and injected s.c. with 300 μl of ice-cold matrigel (BD Biosciences) premixed with 40 μ/ml heparin and 50 μl of CM^{+Gal} (n = 5 mice), CM^{-Gal} (n = 4), CM^{NKT} (n = 4) or CM^{DC} (n = 5). Negative controls (n = 5) were injected with 300 μl matrigel, 40 μ/ml heparin, and 50 μl of serum-free medium. After 7 d, mice were euthanized by CO_2 asphyxia and cervical dislocation. Matrigel plugs were removed, placed in OCT cryomatrix and snap frozen in liquid nitrogen for further analysis. Frozen sections (7 μm) of the matrigel plugs were stained with CD31-phycoerythrin (PE) antibody (R&D Systems, Abingdon, UK) and DAPI (Invitrogen, Gent, Belgium) and photographed on Nikon Eclipse TE2000E inverted fluorescence microscope (Nikon Belux, Brussels, Belgium). ECs were counted as number of nuclei inside the PE fluorescence in two sections per sample.

Murine endothelial cell line cultures

Two EC lines were used; the BM EC line, STR-10, and the brain EC line, bEnd.3. STR-10 (a gift from Dr. Kobayashi, Laboratory of Pathology, Cancer Institute, Hokkaido University School of Medicine, Japan) was previously established by transfecting primary EC cultures with SV40, and immortalized cells were selected (Imai *et al*, 1999), whereas bEnd.3 (a gift from Dr. Y. St-Pierre, Immunology Research Center, Institut Armand-Frappier, Québec, Canada) was established from polyoma-induced brain haemangiomas (Hahne *et al*, 1993). The ECs were cultured in RPMI-1640 supplemented medium with 10% FCS and incubated at 37°C in a humidified 5% CO_2 incubator (Aoudjit *et al*, 1998; Imai *et al*, 1999). After reaching confluence, cells were detached with 0·05% trypsin-EDTA (Gibco, Gent, Belgium).

Cell viability and proliferation assays

For *in vitro* studies, STR-10 and bEnd.3 cells were plated out (1000 cells per well) in triplicate in RPMI-1640 medium

supplemented with 10% FCS in 96-well plates. Once they had grown to approximately 70% confluence, the cells were starved for 24 h. CM and controls were added for another 48 h. Cell Titer-Glo (Promega, Leiden, The Netherlands) and bromodeoxyuridine (BrdU) cell proliferation (Cell Signaling Technology, Leiden, The Netherlands) assays were performed separately according to the manufacturer's instructions. Briefly, proliferation was determined by adding BrdU to the culture for 4 h, then the cells were fixed, denatured and BrdU detection performed with a mouse monoclonal antibody (mAb) and quantified by measuring the absorbance at 450 nm.

Wound healing assay

STR-10 cells ($\approx 30 \times 10^3$/well) were grown in 24-well plates in RPMI-1640 medium supplemented with 10% FCS until they reached 70–80% confluence. Then, the cells were treated with 10 μg/ml mitomycin C (Sigma, Saint Louis, MO, USA) in RPMI-1640 medium supplemented with 5% FCS to inhibit cell proliferation. After 1 h, wounds were made by horizontally scraping the cell monolayers with P200 pipette tips and floating cells were removed by extensive washing with cold PBS. CM and controls were added and the migration distance was recorded immediately (0 time point) and 24 h after scratching, using a Nikon Eclipse TE2000E inverted fluorescence microscope (Nikon). The empty area along each wound was measured after tracing the wound margins using an image analysis program (ImageJ; National Institutes of Health, Bethesda, MD, USA). The percentage of migration area was calculated as follows: (area of original wound – area of actual wound) × 100/area of original wound.

In vitro *matrigel capillarogenesis assay*

STR-10 cells ($\approx 10 \times 10^3$/well) were plated on matrigel-coated (BD Biosciences) 96-well plates (Greiner bio-one, Wemmel, Belgium) specific for confocal imaging and treated with CM or control media. After 16–18 h, the skeletonizations of the network were examined and photographed using a Nikon Eclipse TE2000E inverted fluorescence microscope (Nikon). Each experiment was performed in triplicate and the 3-dimensional network organization was quantified using the ImageJ program. The 'mesh areas' were considered as the surface of empty regions of the field delimited by tubules and cell clusters and were calculated as a percentage of the total area.

Apoptosis assay using terminal deoxynucleotidyl transferase dUTP nick end labelling (TUNEL) staining

After *in vitro* matrigel capillarogenesis assay, cells were fixed with 2% paraformaldehyde for 20 min at 4°C and permeabilized with 0·2% Triton X-100 for 10 min at room temperature. To detect apoptosis, cells were stained using a TUNEL staining method according to the manufacturer's instructions (DeadEnd™ Fluorometric TUNEL System; Promega). Briefly, cells were incubated in a mixture containing terminal deoxynucleotidyl transferase and fluorescein-12-dUTPs for 1 h at 37°C. Then, cells were counterstained with Hoechst 33258. Cells were photographed using a Multiphoton Laser-Scanning confocal microscope (LSM710 and Confocal 3 System, Zeiss, Oberkochen, Germany). The total number of TUNEL-positive cells and counter-stained positive cells were individually counted in 2 areas from each well. The percentage of apoptotic cells was calculated compared to the total number of cells.

Western blot

STR-10 and bEnd.3 cells were cultured in different CM and control media at $0{\cdot}5 \times 10^6$/500 μl. After 10- and 48-h, cell pellets were harvested, lysed in lysis buffer containing different protease and phosphatase inhibitors and Western blotting performed as previously described (Menu *et al*, 2004). Primary Abs against CASP3 (caspase 3; 8G10), STAT1, p-STAT1 (Tyr701) (58D6), STAT3 (79D7), p-STAT3 (Tyr705) (3E2), JAK1, p-JAK1 (Tyr1022/1023), JAK2 (D2E12) XP®, p-JAK2 (Tyr1007/1008) (C80C3), and IRF1 (D5E4) XP® were incubated with blotted samples overnight at 4°C. Membranes were reprobed with ACTB (β-actin). HRP-coupled secondary Ab (anti-rabbit or anti-mouse) was used and bands were visualized using the enhanced chemiluminescence (ECL) system (Amersham, Diegem, Belgium). All Abs were purchased from Cell Signaling Technology.

Statistical analysis

Differences between groups were determined by a Mann–Whitney and Student's *t* test wherever relevant. *P*-values $<0{\cdot}05$ were considered as significant.

Results

Effect of α-GalCer treatment on MM-induced angiogenesis

To determine whether α-GalCer treatment could directly affect angiogenesis in the 5T33MM mice, 2 μg of α-GalCer was injected i.p. at 4-d intervals, beginning on the same day of MM inoculation. Administration of α-GalCer significantly reduced both the serum M-protein concentration, from $21{\cdot}8 \pm 3{\cdot}1$ g/l in vehicles to $5{\cdot}3 \pm 2{\cdot}4$ g/l in the α-GalCer treated group (Fig 1A), and BM tumour load, from $68{\cdot}22 \pm 5{\cdot}03\%$ in vehicles to $22 \pm 7{\cdot}91\%$ in the α-GalCer treated group (Fig 1B). We further measured the MVD in the BM and found that it was significantly reduced in the α-GalCer treated group ($23{\cdot}7 \pm 0{\cdot}93\%$) compared to the vehicles ($33{\cdot}33 \pm 1{\cdot}32\%$) (Fig 1C). Interestingly, the MVD was

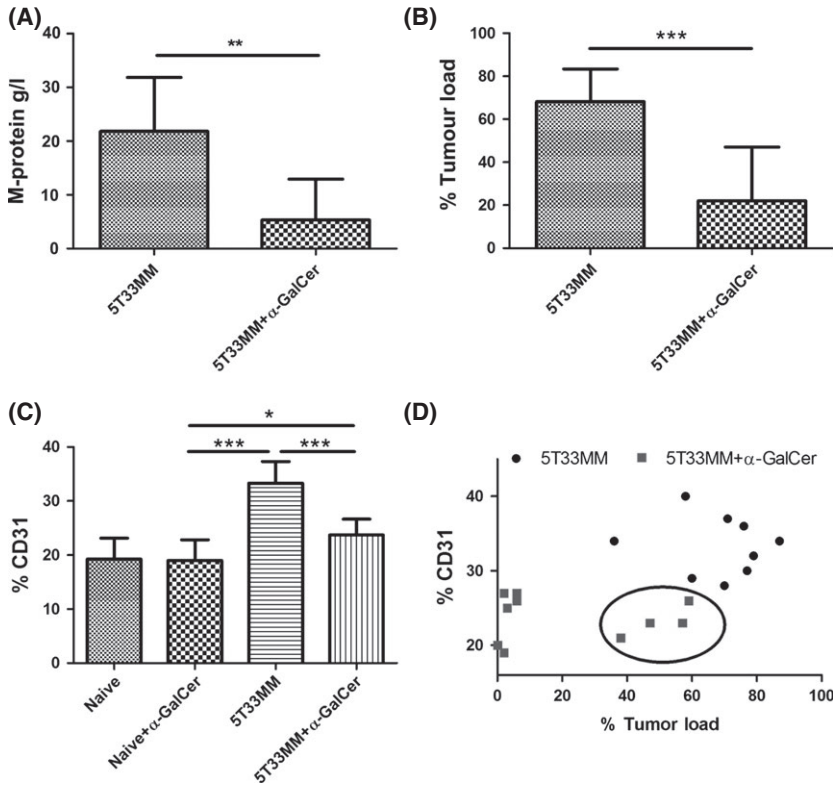

Fig 1. The effect of α-GalCer administration on multiple myeloma development and tumour angiogenesis. C57B1/KaLwRij mice were inoculated with 5T33MM cells and injected i.p. with α-GalCer or vehicle on the same day of inoculation and then at 4-d intervals. (A) M-protein concentration (g/l) as determined by serum protein electrophoresis. (B) Tumour load was assessed on May-Grünwald Giemsa stained cytosmears obtained from the isolated bone marrow (BM). (C) Microvessel density (MVD; % CD31 positive-cells) in the BM. All data represent the mean ± SD of 10 mice in each group (*$P < 0{\cdot}05$, **$P < 0{\cdot}005$ and ***$P < 0{\cdot}001$). (D) Representative scatter blot of MVD versus tumour load using the values obtained from 5T33MM mice treated or not with α-GalCer.

also reduced in the mice with high tumour load (Fig 1D). However, a significant difference, albeit small, persisted between the naïve and MM group (19 ± 1·70% vs. 23·7 ± 0·93%) when both were treated with α-GalCer. We also observed that IFN-γ was secreted early in response to α-GalCer injection (mean = 4·42 ng/ml on week 1) and gradually declined during the progression of the disease (2·18 and 1·04 ng/ml at week 2 and 3, respectively). These data suggest that α-GalCer treatment can be used in the 5T33MM model as an anti-angiogenic co-therapy. As α-GalCer is the activator of iNKT cells, we assumed that α-GalCer-activated iNKT cells might play a significant role in the inhibition of angiogenesis in the 5T33MM model.

Conditioned medium of activated iNKT cells reduces neovascularization in CAM and matrigel plug assays

To further assess the involvement of α-GalCer-activated iNKT cells in angiogenesis, we first prepared CM of α-GalCer-stimulated iNKT cells (CM^{+Gal}). This CM contained, on average, 2·03 ng/ml IFN-γ as measured by enzyme-linked immunosorbent assay (ELISA) and was then used to first examine the effects of iNKT cells *in vivo* in the CAM assay. CAMs were implanted with a gelatine sponge soaked with CM^{+Gal} or controls. Newly-formed blood capillaries, converging radially toward the sponge in a 'spoked-wheel' pattern, were fewer in CM^{+Gal} (mean vessel count = 13 ± 3) compared to CM^{-Gal} (26 ± 3), CM^{NKT} (27 ± 3) and CM^{DC} (25 ± 4) (Fig 2A,C). Next, we performed a matrigel plug assay in NOD-*scid* mice using injected matrigel mixed with CM and angiogenesis was quantified within the explanted plugs after 7 d. A significant reduction of microvascular count was clearly seen in CM^{+Gal} ($CD31^+$ cell count = 25 ± 8) compared to CM^{-Gal} (112 ± 14), CM^{NKT} (93 ± 9) and CM^{DC} (85 ± 11) (Fig 2B,D). The significant reduction in neovascularization observed with CM^{+Gal} confirms the role of activated iNKT cells in angiogenesis, and indicates that the soluble mediators secreted by α-GalCer-activated iNKT cells in the CM^{+Gal} were involved in this process. As CM^{+Gal} contains large amounts of IFN-γ, this cytokine is most probably involved in the inhibition of angiogenesis.

Inhibition of proliferation, migration and tube formation in murine endothelial cell lines

To investigate the potential mechanisms by which activated iNKT cells can affect EC functions, and to determine whether IFN-γ secreted by the activated iNKT cells contributes in the angiostatic processes, STR-10 and bEnd.3 EC lines were examined *in vitro*. First, we checked whether CM could affect the viability of ECs. The cell lines were cultured in CM and controls for 48 h and then the Cell Titer-Glo assay was performed. We found a significant reduction in the viability of both STR-10 and bEnd.3 cells treated with 50 ng/ml rIFN-γ or with CM^{+Gal} compared to control (Fig 3A). The ECs viability was partially, but significantly rescued by 10 μg/ml IFN-γ Ab added to the CM^{+Gal}. Other CM had little or no

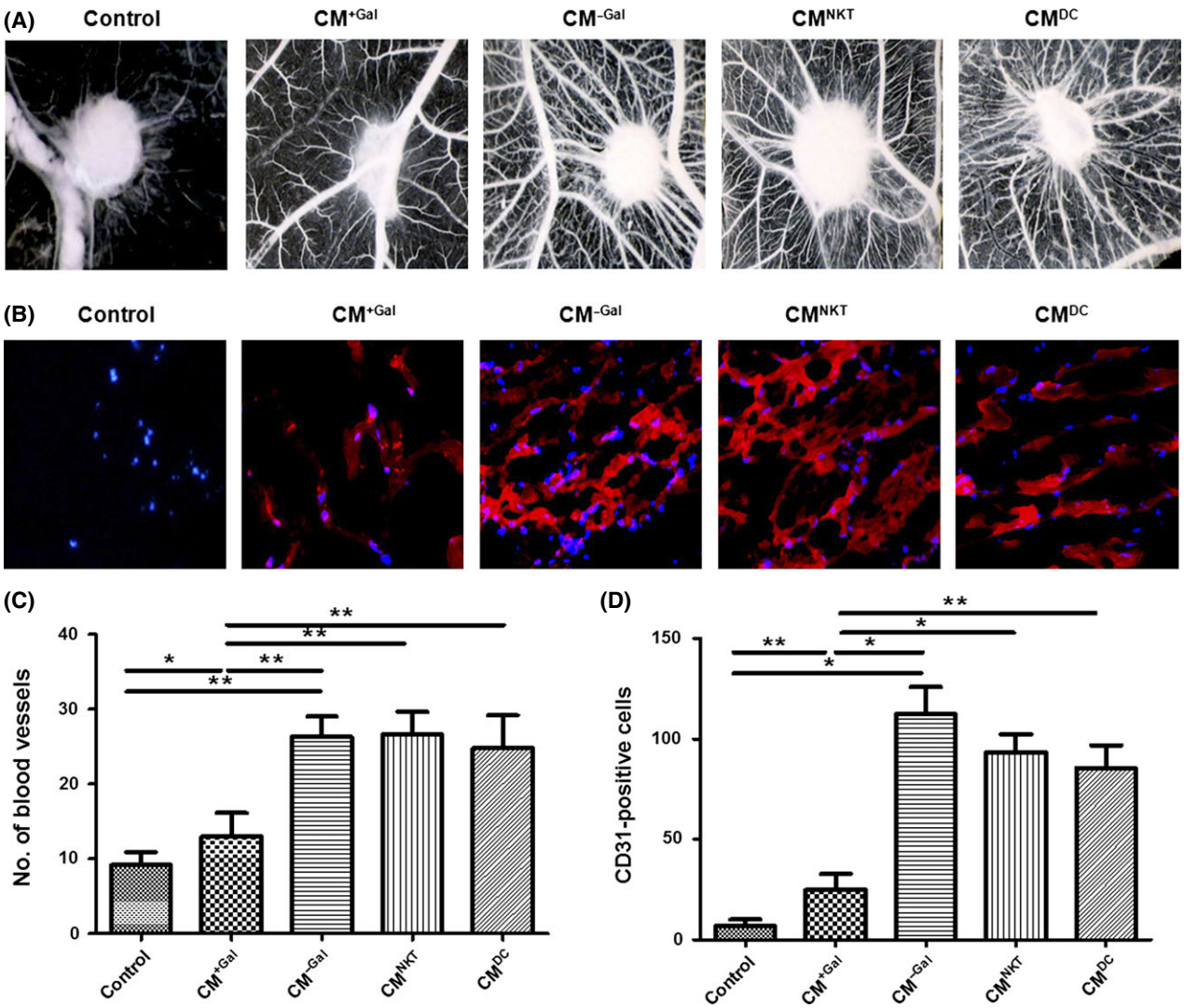

Fig 2. *In vivo* angiogenesis assays showing the impact of CM from stimulated iNKT cells on neovascularisation. (A) Representative pictures (×50) of the chick chorioallantoic membrane (CAM) assay of a fertilized chick embryo. (B) Representative pictures (×400) of the matrigel plug assay as assessed by CD31 staining. (C) Bar graph showing the number of vessels sprouting out in the CAM assay, counted by light and dark field microscopy. (D) Bar graph showing the number of CD31-positive cells, counted by fluorescence microscopy. Values are represented as the mean ± SD, $n = 3$ (*$P < 0{\cdot}05$, **$P < 0{\cdot}005$). iNKT cells, invariant natural killer T cells; CM, conditioned media.

effect. Next we wanted to determine whether this reduction in viability was related to decreased proliferation or survival. Using a BrdU assay, there was a significant reduction (≈50%) in the proliferation of both STR-10 and bEnd.3 cells exposed to CM^{+Gal}, and rIFN-γ reduced growth more apparently in STR-10 cells (Fig 3B). Addition of 10 μg/ml IFN-γ Ab to CM^{+Gal} almost completely restored the growth of ECs, implying that activated iNKT cells can partially block EC proliferation via the IFN-γ pathway. We next examined the migratory capacity of STR-10 cells by an *in vitro* migration and matrigel capillarogenesis assays. Using a 'wound healing' assay we found that CM^{+Gal} could significantly reduce migration after 24 h (% of EC migration = 46 ± 6·7 compared to 56% in control and CM^{-Gal}) (Fig 3C,D). The IFN-γ Ab could only block this reduction by 25%. This indicates that IFN-γ is not the main cytokine involved in the anti-migratory activity of iNKT cells and implies the contribution of other factors secreted by activated iNKT cells in this process. The matrigel capillarogenesis assay was then performed to investigate the morphological defects that could be induced by the CM from activated iNKT cells. After a 16- to 18-h incubation, CM^{+Gal} was shown to induce more non-structured cell clumps throughout the matrigel surface with less branching and poorly organized capillary-like structures (Fig 4A). In these clumps, ECs are clustered and densely packed together, making the connections wider than normal vessels and suggesting an arrest of the differentiation into network vessels. To quantify this defect, the mesh area was summarized for each condition, defined as the empty region

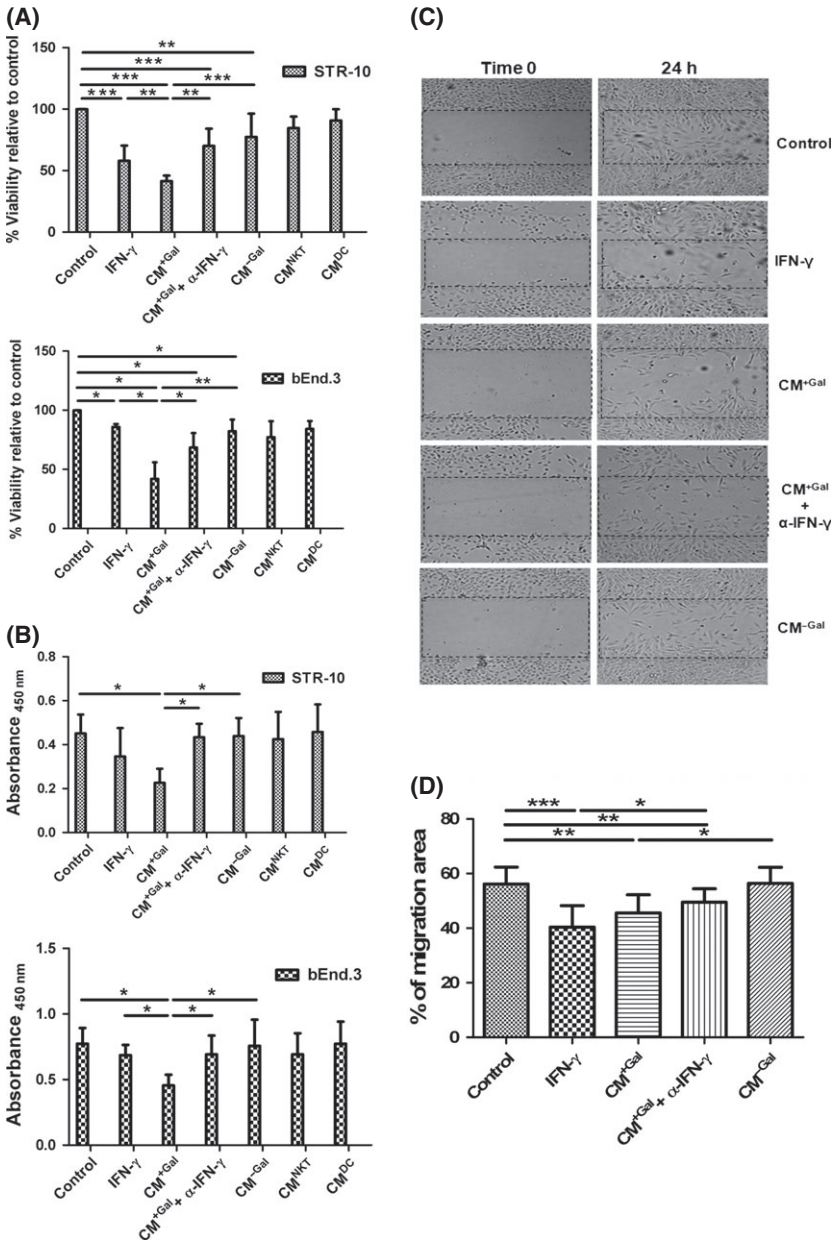

Fig 3. *In vitro* angiogenesis assays. (A) Effect of CM from stimulated iNKT cells on the cell viability of STR-10 (top) and bEnd.3 (bottom) cells as measured by the Cell Titer-Glo assay after 48-h culture. Results are given relative to control and represented as the mean ± SD of 5 independent experiments. (B) Inhibition of STR-10 (top) and bEnd.3 (bottom) cell proliferation by CM from stimulated iNKT cells as measured by BrdU incorporation after 48-h culture. The mean ± SD of 5 independent experiments are shown. (*$P < 0{\cdot}05$, **$P < 0{\cdot}01$ and ***$P < 0{\cdot}0005$). (C) A representative image for each condition is shown at time 0 and after 24-h culture highlighting the difference between the original and final wound space. (D) The wound closure was estimated using ImageJ software, by tracing the wound margins at time 0 and 24 h, and by quantifying the migration area as a percentage of the original wound size. Data (% of the migrated area after 24 h) from 3 independent experiments are presented in the bar graph (*$P < 0{\cdot}05$, **$P < 0{\cdot}01$ and ***$P < 0{\cdot}0005$). iNKT cells, invariant natural killer T cells; CM, conditioned media.

delimited by tubules and cell clusters, and we calculated them as a percentage of an assigned total area. We found that the mesh area covered only 7·83% of the total space in CM^{+Gal}, resulting in an inhibition of more than 75% of the net formation compared to control (35·16%). In contrast, the inhibition induced by rIFN-γ did not exceed 25% (Fig 4C). The percentage of the mesh areas was also lowered by ≈62% in CM^{+Gal} compared to CM^{-Gal} (20·78%). Reduction of mesh area formation in CM from stimulated iNKT cells not only confirms the significant role of α-GalCer, but also indicates that IFN-γ secreted by stimulated iNKT cells could interfere with the normal skeletonization of STR-10 cells. This was demonstrated by blocking IFN-γ signaling with an IFN-γ Ab, which increased the percentage of mesh area by ≈70% compared to CM^{+Gal}.

Activation of apoptosis in murine endothelial cell lines in vitro

As CM obtained from α-GalCer-activated iNKT cells has been shown to reduce angiogenesis in EC lines by reducing proliferation, migration and network formation, we wanted to examine if CM^{+Gal} could induce apoptosis in STR-10 cells. To address this, we used the same matrigel capillarogenesis assay to stain for apoptotic cells by means of the TUNEL assay (Fig 4B). Cells positive for TUNEL (pink colour) were significantly increased in CM^{+Gal} (% of apoptotic cells = 31·92 ± 13) compared to control (10·6 ± 7·1%) and CM^{-Gal} (9·71 ± 6·5%) (Fig 4D). The IFN-γ blocking antibody reduced apoptosis in CM^{+Gal} by ≈60%, demonstrating that IFN-γ partially contributes to the increased cell death

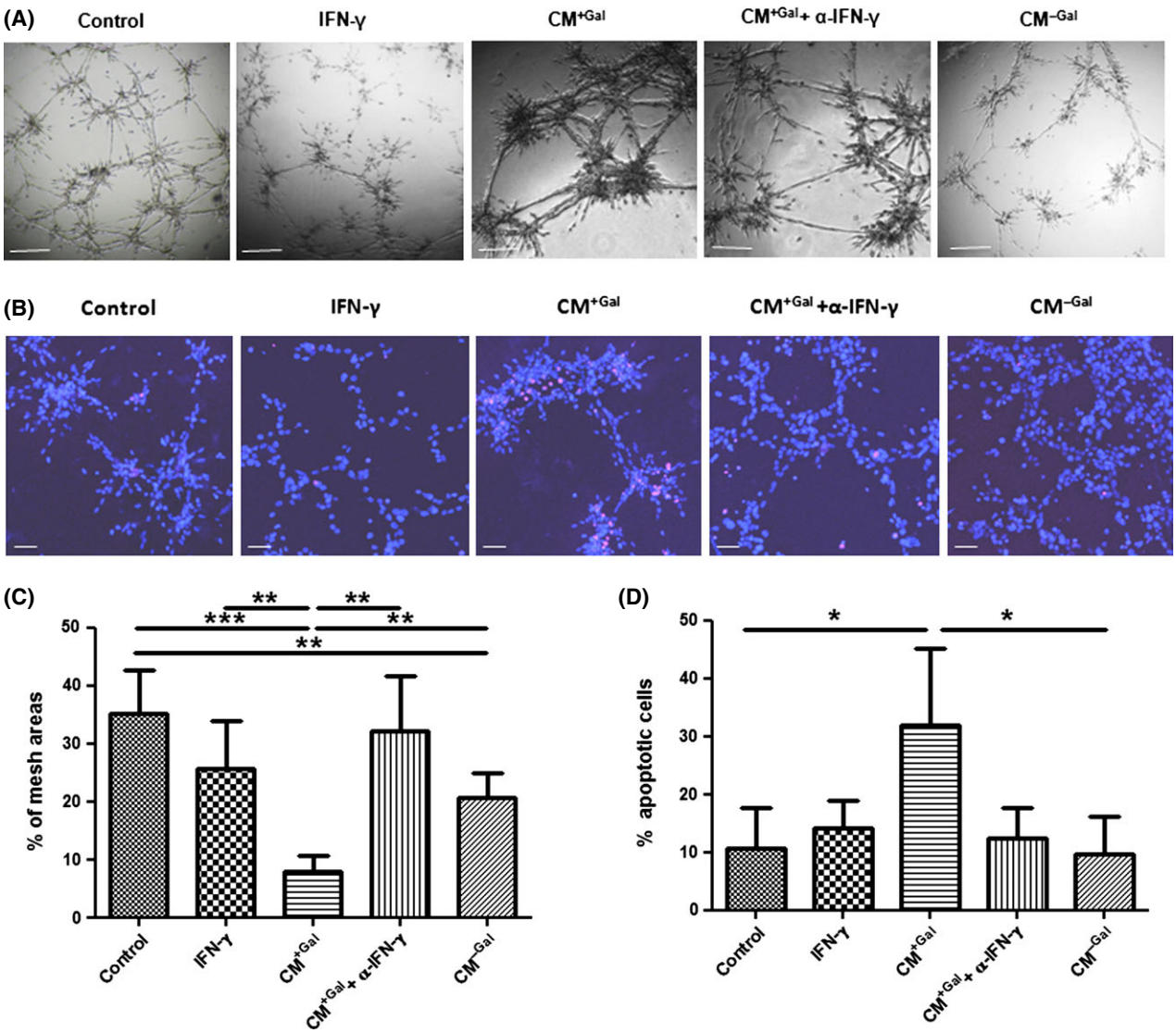

Fig 4. Assessment of skeletonization and apoptosis of STR-10 cells (A) Representative images of network formation in the matrigel capillarogenesis assay, scale bar = 120 μm. (B) Representative images of the number of apoptotic cells (TUNEL positive) induced by CM from stimulated iNKT cells, scale bar = 42 μm. The Z-stacks pictures from each matrigel layer were merged in a single focussed image, using Volocity 5 software. (C) Bar graph of the % of mesh area, defined as the surface of empty regions of the field delimited by tubules and cell clusters. (D) Bar graph representing the % of apoptotic cells relative to the total number of cells. Results are given as mean ± SD (*$P < 0{\cdot}05$, **$P < 0{\cdot}01$ and *** $P < 0{\cdot}0001$, $n = 3$). iNKT cells, invariant natural killer T cells; CM, conditioned media.

and can be suggested as a possible mediator of the apoptotic pathway besides others. We further confirmed the contribution of IFN-γ in this pathway by measuring CASP3 cleavage in Western blot assays. We found that in the two EC lines (STR10 and bEnd.3), both rIFN-γ and CM^{+Gal} increased CASP3 cleavage relative to control, and that this could be partially blocked by an IFN-γ blocking antibody (Fig 5).

Activation of JAK-STAT signalling pathway indicates the role of IFN-γ in angiogenesis

Given that IFN-γ activates the JAK-STAT pathway, which affects different cell functions, such as cell growth, proliferation, migration and apoptosis (Rawlings *et al*, 2004), we sought to confirm the essential role of IFN-γ in the observed anti-angiogenic effects. We therefore analysed STAT1, STAT3, JAK1 and JAK2 phosphorylations by Western blot in STR-10 and bEnd.3 cells treated with CM^{+Gal}. We found that CM^{+Gal} markedly induced P-STAT1, total STAT1 and P-JAK2 in STR-10 (Fig 5A) and bEnd.3 cells (Fig 5B) much more than CM^{-Gal}. CM^{+Gal} also induced JAK1 phosphorylation, but to a lesser extent. Furthermore, we examined the downstream signalling protein IFN-γ regulatory factor-1 (IRF1) and found it was upregulated in CM^{+Gal} when compared to the other conditions. However, the STAT3 activation was not clearly distinguishable between CM^{+Gal} and the other conditions,

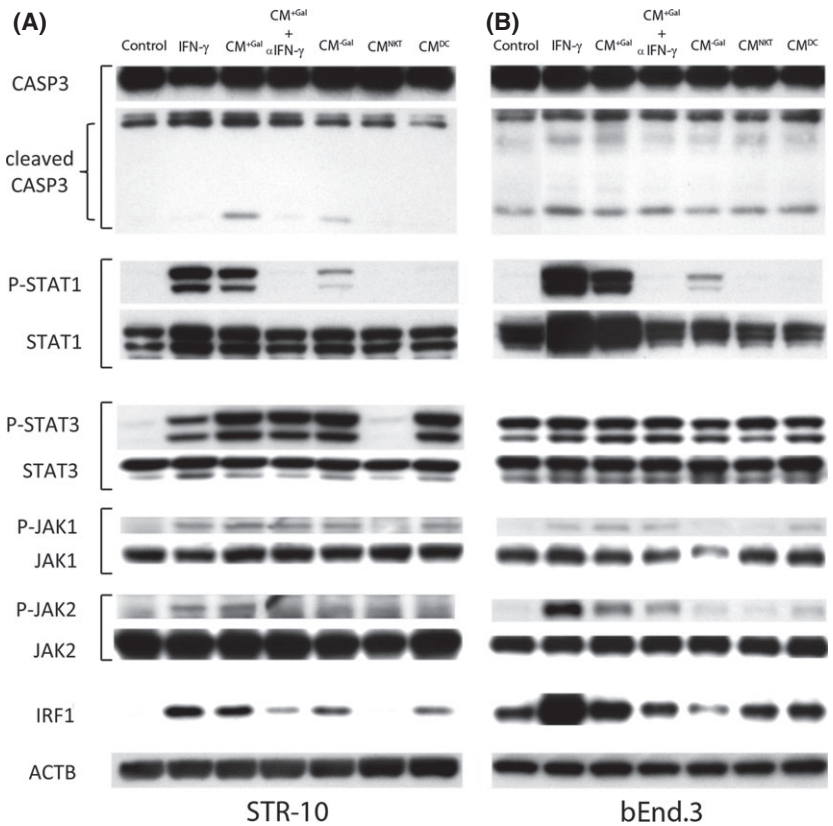

Fig 5. CM from stimulated iNKT cells induces activation of the JAK-STAT pathway and CASP3 activity *in vitro*. Western blot analysis of CASP3 cleavage (after 48 h) and STAT1, STAT3, JAK1, JAK2 and IRF1 activation (after 10 h) in STR-10 (A) and bEnd.3 (B) cells. ACTB (β Actin) is used as a loading control. Blots are representative results from 1 experiment out of 3 performed. iNKT cells, invariant natural killer T cells; CM, conditioned media. P, phosphorylated.

particularly in bEnd.3 cells. Altogether, these data indicate that IFN-γ secreted by α-GalCer-activated iNKT cells activates the JAK-STAT pathway in ECs, thereby affecting angiogenesis.

Discussion

Angiogenesis is a hallmark of cancer (Folkman, 1971). It is described as a prognostic index and an increase of pro-angiogenic factors is a predictor of poor prognosis in MM (Rajkumar *et al*, 2000; Giles, 2002). Hayakawa *et al* (2002) demonstrated that α-GalCer stimulated NKT cells could inhibit tumour-induced angiogenesis in a solid tumour such as B6-derived melanoma by IFN-γ secretion from both iNKT cells and NK cells. We have recently described that in the 5T33MM model and in MM patients, there is a defect in iNKT numbers leading to a defect in IFN-γ production. However, stimulating iNKT cells with α-GalCer during early stages of the disease increased animal survival (Nur *et al*, 2013b). Furthermore, disease progression was reported to be correlated with angiogenesis in this model (Van Valckenborgh *et al*, 2002). In the present study, we wanted to examine whether the anti-tumour effects of α-GalCer are also mediated through anti-angiogenic effects. As many other cells can be activated *in vivo*, we preferred to investigate the direct effects of iNKT cells on murine EC lines *in vitro* to assess their role in MM-related angiogenesis.

We treated 5T33MM mice with α-GalCer during the course of the disease and noticed a clear reduction in tumour load and paraprotein, therefore confirming our previous data (Nur *et al*, 2013b). More importantly, this was associated with a reduction in MVD, even in mice with a higher tumour burden. This indicates that α-GalCer has both direct anti-angiogenic effects and anti-tumour effects.

While analysing the direct effects of iNKT cells on angiogenesis we found that CM of α-GalCer stimulated iNKT cells reduced neovasculogenesis in the CAM and matrigel plug assays *in vivo*, and that it reduced proliferation, migration and network formation, but induced apoptosis of EC lines *in vitro*. This was further confirmed by activation of CASP3 in response to CM^{+Gal}. To further examine the mechanisms underlying these anti-angiogenic effects, we focussed on IFN-γ, which is the predominant cytokine secreted by iNKT cells in response to α-GalCer. It has been reported that α-GalCer-activated human iNKT cells can induce anti-tumour effects via the release of soluble mediators, such as IFN-γ, rather than through the cytolytic toxicity of the cells (Kikuchi *et al*, 2001). This is consistent with the reported findings from the Okumura group (Hayakawa *et al*, 2001). Furthermore, it has been demonstrated that the anti-tumour effect of IFN-γ is partly mediated by inhibition of angiogenesis (Ikeda *et al*, 2002) and that IFN-γ inhibits EC proliferation and vasularization, and induces apoptosis (Ribatti *et al*, 2006). Therefore we assume that IFN-γ is the key mediator in the anti-tumour and anti-angiogenic effects of iNKT cells. This is indeed confirmed by our findings that addition of an IFN-γ blocking Ab reduced the anti-angiogenic effects of CM^{+Gal}. However,

given the stronger effects of CM^{+Gal} versus rIFN-γ, we presume that other mediators derived from activated iNKT cells might work synergistically with IFN-γ. To this end, we performed a cytokine array comparing CM^{+Gal} to CM^{-Gal} to determine whether other anti-angiogenic cytokines were secreted. We found that IFN-γ-inducible protein (IP-10, also known as CXCL10) was also strongly secreted by stimulated iNKT cells (Figure S1A). IP-10 and monokine-induced by IFN-γ (MIG, also known as CXCL9), have been shown to possess potent anti-angiogenic effects *in vivo*, such as the inhibition of basic fibroblast growth factor-induced neovascularization in the murine athymic model (Angiolillo *et al*, 1995; Sgadari *et al*, 1996). IP-10 was also described to exert angiostatic effects in different xenograft models (Arenberg *et al*, 1996; Feldman *et al*, 2002; Yang & Richmond, 2004). However, the direct addition of IP-10 to the culture, did not result in any anti-angiogenic effects on STR-10 or bEnd.3 cells (Figure S1B), which is in contrast with the result reported by Campanella *et al* (2010), who showed anti-proliferative effects of IP-10 on ECs isolated from different organs. This could be due to a low expression of IP-10 receptor (CXCR3) on the STR-10 and bEnd.3 cells. Other possible cytokines with angiostatic activity are interleukin (IL) 12 and IL18, which are known to synergize to induce IFN-γ production by T cells and many studies indicated that their anti-tumour and angiostatic activities are IFN-γ-dependent (Nastala *et al*, 1994; Voest *et al*, 1995; Coughlin *et al*, 1998; Cao *et al*, 1999; Ikeda *et al*, 2002). In addition, IL12 has been shown to inhibit EC activities, such as proliferation, in an IFN-γ-dependent way (Strasly *et al*, 2001; Hayakawa *et al*, 2002). As DCs are IL12 producers, we suppose that IL12 triggers IFN-γ secretion by α-GalCer-activated iNKT cells and this would amplify the anti-angiogenic loops mediated by IFN-γ.

Further supporting the hypothesis that IFN-γ is a key mediator of the anti-angiogenic activity of iNKT cells, is the observation that the JAK-STAT signalling pathway, including STAT1, JAK2 and IRF1, is strongly activated in ECs when cultured in CM^{+Gal}. In response to IFN-γ, STAT1 is highly activated and freely translocates to the nucleus to bind Gamma Activating Sequence (GAS) to initiate several primary response genes such as *IRF1* (Kerr *et al*, 2003; Saha *et al*, 2010). *IRF1* is involved in stimulating other IFN-γ-inducible genes, such as *NOS2* (nitric oxide synthase 2, inducible), which can also impair angiogenesis (Mayo *et al*, 2014). IRF1 can furthermore trigger IL12 secretion and IL12 receptor, which, leads to restimulation by IFN-γ and IRF1 in an autocrine manner (Saha *et al*, 2010). We also observed a slight activation of STAT1 in CM^{-Gal} conditions. This can be explained by the fact that unstimulated iNKT cells also produce small amounts of IFN-γ (200 pg/ml). Although JAK1 is also required in IFN-γ receptor signalling (Kerr *et al*, 2003; Schindler *et al*, 2007), we could not detect high activation of JAK1 compared to STAT1 and JAK2. Instead, JAK1 and STAT3 are known to play major roles in IL6 responses (Kerr *et al*, 2003; Schindler *et al*, 2007). We found through the cytokine array that IL6 was present in both CM^{+Gal} and CM^{-Gal} in similar measures. Therefore, activation of STAT3 and JAK1 in these conditions is most likely a response to IL6. In conclusion, we found that activation of the JAK-STAT pathway in an IFN-γ-dependent manner is the most likely mechanism through which activated iNKT cells exert their anti-angiogenic effects. Moreover, activation of this pathway has also been shown to promote apoptosis of EC through activation of caspases or Fas/FasL (Li *et al*, 2002). The upregulation of IRF1 observed in CM^{+Gal} can induce proapoptotic activity through caspases (Chin *et al*, 1997; Schroder *et al*, 2004). In our study, we detected apoptotic activity when EC were cultured in CM^{+Gal}, as we clearly observed more TUNEL-positive ECs. On the other hand, CASP3 cleavage was only slightly enhanced, indicating the involvement of other death-linked mechanisms.

From a clinical point of view, there has been great interest in anti-angiogenic therapy for MM patients. Several angiogenesis inhibitors have been discovered and used as a single agent or in combination with chemotherapy in cancer (Daly *et al*, 2003; Grepin & Pages, 2010). These inhibitors can target vascular endothelial growth factor (VEGF) (e.g., Bevacizumab) or their receptors (e.g., tyrosine kinase inhibitors, such as Sorafenib tosylate and Sunitinib malate), and have been investigated in different clinical trials of solid tumours (Grepin & Pages, 2010). Also for MM, VEGF-neutralizing mAbs and tyrosine kinase inhibitors have been approved (Medinger & Mross, 2010). Unfortunately, these anti-angiogenesis therapies significantly reduced tumour progression, but did not induce tumour regression and in many cases, patients only responded transiently. In addition, few studies reported an increase in thrombotic or haemorrhagic complications in some patients following these treatments (Daly *et al*, 2003). Therefore, treatments that have a broader effect are preferred. In MM, the immunomodulatory drug, lenalidomide, is now widely used as a first line therapy. Besides having potent immune-stimulating effects executed by increasing conventional T cell functions, DC activation, NKT cell co-stimulation, NK cell cytotoxicity and decreasing regulatory T cell functions (Davies *et al*, 2001; Marriott *et al*, 2002; Chang *et al*, 2006; Song *et al*, 2008; Galustian *et al*, 2009; Quach *et al*, 2010; De Keersmaecker *et al*, 2012; Mitsiades & Chen-Kiang, 2013), lenalidomide has also been shown to efficiently reduce migration and vessel formation of ECs isolated from patients with active MM while having no effect on their proliferation or apoptosis (Lu *et al*, 2009; De Luisi *et al*, 2011). It also reduces the expression of pro-angiogenic factors, such as VEGF and IL6 (Medinger & Mross, 2010). Similarly, another promising immunomodulatory drug, pomalidomide, has been shown to inhibit angiogenesis in MM by reducing VEGF and hypoxia-inducible factor 1 (Chanan-Khan *et al*, 2013).

Administration of free α-GalCer has shown promising antitumour effects in murine models. However, its clinical use has been limited by the hyporesponsiveness of the iNKT cells. A possible explanation is the development of an uncontrolled

response given the uncertainty about the cells that pick up the α-GalCer (Macho-Fernandez *et al*, 2014). The use of α-GalCer-loaded DCs can overcome this problem and was shown to be more potent (Chang *et al*, 2005). In a preclinical melanoma model, Macho-Fernandez *et al* (2014) examined the delivery of encapsulated α-GalCer together with ovalbumin antigens in poly(lactic-co-glycolic acid) -based particles, directed to DCs. This vaccine triggered more specific adaptive responses (Macho-Fernandez *et al*, 2014). Similarly, Hong *et al* (2013) examined the effects of using α-GalCer-loaded MOPC315BM myeloma cells as a vaccine in a murine MM model. The vaccine induced expansion and activation of iNKT cells, and promising therapeutical responses were detected. Interestingly, in a recent clinical report, 3 out of 4 asymptomatic MM patients who received lenalidomide together with autologous α-GalCer-loaded DCs experienced a reduction in monoclonal immunoglobulin and an expansion of neutrophils, monocytes and NK cells in the peripheral circulation (Richter *et al*, 2013). These data demonstrate the possible use of (vectorized) α-GalCer in MM patients. Furthermore, activation of iNKT cells can be combined with established anti-MM drugs, such as bortezomib, which has been shown to mediate strong anti-tumour effects together with potent anti-angiogenic effects in MM patient-derived ECs by down regulating VEGF, IL6, angiopoietin 1 and 2 (Roccaro *et al*, 2006). Combination therapy has the advantage of activating the immune system at a time when tumour burden is low. In summary, we found that activating iNKT cells with α-GalCer not only has strong anti-tumour effects, but it also has promising anti-angiogenic actions. Therefore iNKT cell stimulation is a good candidate for complementary combination therapies, which could lead to novel treatment regimens for MM patients.

Acknowledgements

We thank Carine Seynaeve, Sofie Seghers, Marie Joos de ter Beerst and Eddy Himpe for their expert technical assistance. We also thank the Clinical Chemistry laboratory (UZ Brussel), headed by Prof. Gorus, for the measurement of M-protein levels. E. Menu, E. Van Valckenborgh and E. De Bruyne are postdoctoral fellows of FWO-VI.

Author contributions

HN: performed and designed the research, analysed the data, wrote and revised the manuscript; LR: performed the research, analysed the data, wrote and revised the manuscript; MAF and DR: designed the research, analysed the data and revised the manuscript; HDR and JKM: performed the research, analysed the data and revised the manuscript; EVV, EDB, AV and KV: designed the research and revised the manuscript; EM: designed the research, analysed the data, wrote and revised the manuscript.

Funding

This work was financially supported by the Vlaams Liga tegen Kanker (VLK), FWO-Vl and the European Commission Framework of the Erasmus Mundus External Cooperation Window under grant agreement 2009-1642/001-001-ECW. It was also supported by Associazione Italiana per la Ricerca sul Cancro (AIRC, Milan), Investigator grant (no. 14095) and the 5 per thousand Molecular Clinical Oncology Special Program (grant no. 9965) to AV and the European Union Seventh Framework Programme (FP7/2007- 2013) under grant agreement no 278570 to DR. The funders have no role in study design, data collection and analysis, decision to publish, or preparation of the manuscript.

Supporting Information

Additional Supporting Information may be found in the online version of this article:

Fig S1. Effect of IP-10 on EC lines. (A) Cytokine array to show some of the secretory products of CM+Gal and CM-Gal. (B) Testing IP-10 on the viability of STR-10 and bEnd.3 cells after 48 h using cell Titer-Glo assay. The mean ± SD of 3 independent experiments is shown.

References

Angiolillo, A.L., Sgadari, C., Taub, D.D., Liao, F., Farber, J.M., Maheshwari, S., Kleinman, H.K., Reaman, G.H. & Tosato, G. (1995) Human interferon-inducible protein 10 is a potent inhibitor of angiogenesis in vivo. *The Journal of Experimental Medicine*, **182**, 155–162.

Aoudjit, F., Potworowski, E.F. & St-Pierre, Y. (1998) Bi-directional induction of matrix metalloproteinase-9 and tissue inhibitor of matrix metalloproteinase-1 during T lymphoma/endothelial cell contact: implication of ICAM-1. *Journal of Immunology*, **160**, 2967–2973.

Arenberg, D.A., Kunkel, S.L., Polverini, P.J., Morris, S.B., Burdick, M.D., Glass, M.C., Taub, D.T., Iannettoni, M.D., Whyte, R.I. & Strieter, R.M. (1996) Interferon-gamma-inducible protein 10 (IP-10) is an angiostatic factor that inhibits human non-small cell lung cancer (NSCLC) tumorigenesis and spontaneous metastases. *The Journal of Experimental Medicine*, **184**, 981–992.

Bhutani, M., Turkbey, B., Tan, E., Kemp, T.J., Pinto, L.A., Berg, A.R., Korde, N., Minter, A.R., Weiss, B.M., Mena, E., Lindenberg, L., Aras, O., Purdue, M.P., Hofmann, J.N., Steinberg, S.M., Calvo, K.R., Choyke, P.L., Maric, I., Kurdziel, K. & Landgren, O. (2014) Bone marrow angiogenesis in myeloma and its precursor disease: a prospective clinical trial. *Leukemia*, **28**, 413–416.

Brennan, P.J., Brigl, M. & Brenner, M.B. (2013) Invariant natural killer T cells: an innate activation scheme linked to diverse effector functions. *Nature Reviews Immunology*, **13**, 101–117.

Campanella, G.S., Colvin, R.A. & Luster, A.D. (2010) CXCL10 can inhibit endothelial cell proliferation independently of CXCR3. *PLoS One*, **5**, e12700.

Cao, R., Farnebo, J., Kurimoto, M. & Cao, Y. (1999) Interleukin-18 acts as an angiogenesis and tumor suppressor. *FASEB Journal*, **13**, 2195–2202.

Cerundolo, V., Silk, J.D., Masri, S.H. & Salio, M. (2009) Harnessing invariant NKT cells in vaccination strategies. *Nature Reviews Immunology*, **9**, 28–38.

Chanan-Khan, A.A., Swaika, A., Paulus, A., Kumar, S.K., Mikhael, J.R., Rajkumar, S.V., Dispenzieri, A. & Lacy, M.Q. (2013) Pomalidomide: the new immunomodulatory agent for the treatment of multiple myeloma. *Blood Cancer journal*, **3**, e143.

Chang, D.H., Osman, K., Connolly, J., Kukreja, A., Krasovsky, J., Pack, M., Hutchinson, A., Geller, M., Liu, N., Annable, R., Shay, J., Kirchhoff, K., Nishi, N., Ando, Y., Hayashi, K., Hassoun, H., Steinman, R.M. & Dhodapkar, M.V. (2005) Sustained expansion of NKT cells and antigen-specific T cells after injection of alpha-galactosyl-ceramide loaded mature dendritic cells in cancer patients. *The Journal of Experimental Medicine*, **201**, 1503–1517.

Chang, D.H., Liu, N., Klimek, V., Hassoun, H., Mazumder, A., Nimer, S.D., Jagannath, S. & Dhodapkar, M.V. (2006) Enhancement of ligand-dependent activation of human natural killer T cells by lenalidomide: therapeutic implications. *Blood*, **108**, 618–621.

Chin, Y.E., Kitagawa, M., Kuida, K., Flavell, R.A. & Fu, X.Y. (1997) Activation of the STAT signaling pathway can cause expression of caspase 1 and apoptosis. *Molecular and Cellular Biology*, **17**, 5328–5337.

Coughlin, C.M., Salhany, K.E., Gee, M.S., LaTemple, D.C., Kotenko, S., Ma, X., Gri, G., Wysocka, M., Kim, J.E., Liu, L., Liao, F., Farber, J.M., Pestka, S., Trinchieri, G. & Lee, W.M. (1998) Tumor cell responses to IFNgamma affect tumorigenicity and response to IL-12 therapy and antiangiogenesis. *Immunity*, **9**, 25–34.

Daly, M.E., Makris, A., Reed, M. & Lewis, C.E. (2003) Hemostatic regulators of tumor angiogenesis: a source of antiangiogenic agents for cancer treatment? *Journal of the National Cancer Institute*, **95**, 1660–1673.

Davies, F.E., Raje, N., Hideshima, T., Lentzsch, S., Young, G., Tai, Y.T., Lin, B., Podar, K., Gupta, D., Chauhan, D., Treon, S.P., Richardson, P.G., Schlossman, R.L., Morgan, G.J., Muller, G.W., Stirling, D.I. & Anderson, K.C. (2001) Thalidomide and immunomodulatory derivatives augment natural killer cell cytotoxicity in multiple myeloma. *Blood*, **98**, 210–216.

De Keersmaecker, B., Allard, S.D., Lacor, P., Schots, R., Thielemans, K. & Aerts, J.L. (2012) Expansion of polyfunctional HIV-specific T cells upon stimulation with mRNA electroporated dendritic cells in the presence of immunomodulatory drugs. *Journal of Virology*, **86**, 9351–9360.

De Luisi, A., Ferrucci, A., Coluccia, A.M., Ria, R., Moschetta, M., de Luca, E., Pieroni, L., Maffia, M., Urbani, A., Di Pietro, G., Guarini, A., Ranieri, G., Ditonno, P., Berardi, S., Caivano, A., Basile, A., Cascavilla, N., Capalbo, S., Quarta, G., Dammacco, F., Ribatti, D. & Vacca, A. (2011) Lenalidomide restrains motility and overangiogenic potential of bone marrow endothelial cells in patients with active multiple myeloma. *Clinical Cancer Research*, **17**, 1935–1946.

Dhodapkar, M.V., Geller, M.D., Chang, D.H., Shimizu, K., Fujii, S., Dhodapkar, K.M. & Krasovsky, J. (2003) A reversible defect in natural killer T cell function characterizes the progression of premalignant to malignant multiple myeloma. *The Journal of Experimental Medicine*, **197**, 1667–1676.

Fang, X., Du, P., Liu, Y. & Tang, J. (2010) Efficient isolation of mouse liver NKT cells by perfusion. *PLoS One*, **5**, e10288.

Feldman, A.L., Friedl, J., Lans, T.E., Libutti, S.K., Lorang, D., Miller, M.S., Turner, E.M., Hewitt, S.M. & Alexander, H.R. (2002) Retroviral gene transfer of interferon-inducible protein 10 inhibits growth of human melanoma xenografts. *International Journal of Cancer Journal International du Cancer*, **99**, 149–153.

Folkman, J. (1971) Tumor angiogenesis: therapeutic implications. *The New England Journal of Medicine*, **285**, 1182–1186.

Galustian, C., Meyer, B., Labarthe, M.C., Dredge, K., Klaschka, D., Henry, J., Todryk, S., Chen, R., Muller, G., Stirling, D., Schafer, P., Bartlett, J.B. & Dalgleish, A.G. (2009) The anti-cancer agents lenalidomide and pomalidomide inhibit the proliferation and function of T regulatory cells. *Cancer Immunology, Immunotherapy: CII*, **58**, 1033–1045.

Giles, F.J. (2002) The emerging role of angiogenesis inhibitors in hematologic malignancies. *Oncology*, **16**, 23–29.

Grepin, R. & Pages, G. (2010) Molecular mechanisms of resistance to tumour anti-angiogenic strategies. *Journal of Oncology*, **2010**, 835680.

Hahne, M., Jager, U., Isenmann, S., Hallmann, R. & Vestweber, D. (1993) Five tumor necrosis factor-inducible cell adhesion mechanisms on the surface of mouse endothelioma cells mediate the binding of leukocytes. *The Journal of Cell Biology*, **121**, 655–664.

Hanahan, D. & Folkman, J. (1996) Patterns and emerging mechanisms of the angiogenic switch during tumorigenesis. *Cell*, **86**, 353–364.

Hayakawa, Y., Takeda, K., Yagita, H., Kakuta, S., Iwakura, Y., Van Kaer, L., Saiki, I. & Okumura, K. (2001) Critical contribution of IFN-gamma and NK cells, but not perforin-mediated cytotoxicity, to anti-metastatic effect of alpha-galactosylceramide. *European Journal of Immunology*, **31**, 1720–1727.

Hayakawa, Y., Takeda, K., Yagita, H., Smyth, M.J., Van Kaer, L., Okumura, K. & Saiki, I. (2002) IFN-gamma-mediated inhibition of tumor angiogenesis by natural killer T-cell ligand, alpha-galactosylceramide. *Blood*, **100**, 1728–1733.

Hong, S., Lee, H., Jung, K., Lee, S.M., Lee, S.J., Jun, H.J., Kim, Y., Song, H., Bogen, B. & Choi, I. (2013) Tumor cells loaded with alpha-galactosylceramide promote therapeutic NKT-dependent anti-tumor immunity in multiple myeloma. *Immunology Letters*, **156**, 132–139.

Ikeda, H., Old, L.J. & Schreiber, R.D. (2002) The roles of IFN gamma in protection against tumor development and cancer immunoediting. *Cytokine & Growth Factor Reviews*, **13**, 95–109.

Imai, K., Kobayashi, M., Wang, J., Ohiro, Y., Hamada, J., Cho, Y., Imamura, M., Musashi, M., Kondo, T., Hosokawa, M. & Asaka, M. (1999) Selective transendothelial migration of hematopoietic progenitor cells: a role in homing of progenitor cells. *Blood*, **93**, 149–156.

Jakob, C., Sterz, J., Zavrski, I., Heider, U., Kleeberg, L., Fleissner, C., Kaiser, M. & Sezer, O. (2006) Angiogenesis in multiple myeloma. *European Journal of Cancer*, **42**, 1581–1590.

Kerr, I.M., Costa-Pereira, A.P., Lillemeier, B.F. & Strobl, B. (2003) Of JAKs, STATs, blind watchmakers, jeeps and trains. *FEBS Letters*, **546**, 1–5.

Kikuchi, A., Nieda, M., Schmidt, C., Koezuka, Y., Ishihara, S., Ishikawa, Y., Tadokoro, K., Durrant, S., Boyd, A., Juji, T. & Nicol, A. (2001) In vitro anti-tumour activity of alpha-galactosylceramide-stimulated human invariant Valpha24+NKT cells against melanoma. *British Journal of Cancer*, **85**, 741–746.

Kumar, V. & Delovitch, T.L. (2014) Different subsets of natural killer T cells may vary in their roles in health and disease. *Immunology*, **142**, 321–336.

Li, J.H., Kluger, M.S., Madge, L.A., Zheng, L., Bothwell, A.L. & Pober, J.S. (2002) Interferon-gamma augments CD95(APO-1/Fas) and procaspase-8 expression and sensitizes human vascular endothelial cells to CD95-mediated apoptosis. *The American Journal of Pathology*, **161**, 1485–1495.

Lu, L., Payvandi, F., Wu, L., Zhang, L.H., Hariri, R.J., Man, H.W., Chen, R.S., Muller, G.W., Hughes, C.C., Stirling, D.I., Schafer, P.H. & Bartlett, J.B. (2009) The anti-cancer drug lenalidomide inhibits angiogenesis and metastasis via multiple inhibitory effects on endothelial cell function in normoxic and hypoxic conditions. *Microvascular Research*, **77**, 78–86.

Macho-Fernandez, E., Cruz, L.J., Ghinnagow, R., Fontaine, J., Bialecki, E., Frisch, B., Trottein, F. & Faveeuw, C. (2014) Targeted delivery of alpha-galactosylceramide to CD8alpha+ dendritic cells optimizes type I NKT cell-based antitumor responses. *Journal of Immunology*, **193**, 961–969.

Marriott, J.B., Clarke, I.A., Dredge, K., Muller, G., Stirling, D. & Dalgleish, A.G. (2002) Thalidomide and its analogues have distinct and opposing effects on TNF-alpha and TNFR2 during co-stimulation of both CD4(+) and CD8(+) T cells. *Clinical and Experimental Immunology*, **130**, 75–84.

Matsuda, J.L., Mallevaey, T., Scott-Browne, J. & Gapin, L. (2008) CD1d-restricted iNKT cells, the 'Swiss-Army knife' of the immune system. *Current Opinion in Immunology*, **20**, 358–368.

Mattarollo, S.R., West, A.C., Steegh, K., Duret, H., Paget, C., Martin, B., Matthews, G.M., Shortt, J., Chesi, M., Bergsagel, P.L., Bots, M., Zuber, J., Lowe, S.W., Johnstone, R.W. & Smyth, M.J. (2012) NKT cell adjuvant-based tumor vaccine for treatment of myc oncogene-driven mouse B-cell lymphoma. *Blood*, **120**, 3019–3029.

Mayo, J.N., Chen, C.H., Liao, F.F. & Bearden, S.E. (2014) Homocysteine disrupts outgrowth of microvascular endothelium by an iNOS-dependent mechanism. *Microcirculation*, **21**, 541–550.

Medinger, M. & Mross, K. (2010) Clinical trials with anti-angiogenic agents in hematological

malignancies. *Journal of Angiogenesis Research*, **2**, 10.

Menu, E., Kooijman, R., Van Valckenborgh, E., Asosingh, K., Bakkus, M., Van Camp, B. & Vanderkerken, K. (2004) Specific roles for the PI3K and the MEK-ERK pathway in IGF-1-stimulated chemotaxis, VEGF secretion and proliferation of multiple myeloma cells: study in the 5T33MM model. *British Journal of Cancer*, **90**, 1076–1083.

Menu, E., De Leenheer, E., De Raeve, H., Coulton, L., Imanishi, T., Miyashita, K., Van Valckenborgh, E., Van Riet, I., Van Camp, B., Horuk, R., Croucher, P. & Vanderkerken, K. (2006) Role of CCR1 and CCR5 in homing and growth of multiple myeloma and in the development of osteolytic lesions: a study in the 5TMM model. *Clinical & Experimental Metastasis*, **23**, 291–300.

Mitsiades, C.S. & Chen-Kiang, S. (2013) Immunomodulation as a therapeutic strategy in the treatment of multiple myeloma. *Critical Reviews in Oncology/Hematology*, **88**, S5–S13.

Moehler, T.M., Hillengass, J., Goldschmidt, H. & Ho, A.D. (2004) Antiangiogenic therapy in hematologic malignancies. *Current Pharmaceutical Design*, **10**, 1221–1234.

Nakagawa, K., Iwabuchi, K., Ogasawara, K., Ato, M., Kajiwara, M., Nishihori, H., Iwabuchi, C., Ishikura, H., Good, R.A. & Onoe, K. (1997) Generation of NK1.1+ T cell antigen receptor alpha/beta+ thymocytes associated with intact thymic structure. *Proceedings of the National Academy of Sciences of the United States of America*, **94**, 2472–2477.

Nastala, C.L., Edington, H.D., McKinney, T.G., Tahara, H., Nalesnik, M.A., Brunda, M.J., Gately, M.K., Wolf, S.F., Schreiber, R.D., Storkus, W.J. & Lotze, M.T. (1994) Recombinant IL-12 administration induces tumor regression in association with IFN-gamma production. *Journal of Immunology*, **153**, 1697–1706.

Neparidze, N. & Dhodapkar, M.V. (2009) Harnessing CD1d-restricted T cells toward antitumor immunity in humans. *Annals of the New York Academy of Sciences*, **1174**, 61–67.

Nur, H., Elewaut, D., Vanderkerken, K. & Menu, E. (2013a) The Role of Invariant Natural Killer T cells in Cancer. *International Blood Research & Reviews*, **1**, 44–71.

Nur, H., Fostier, K., Aspeslagh, S., Renmans, W., Bertrand, E., Leleu, X., Favreau, M., Breckpot, K., Schots, R., De Waele, M., Van Valckenborgh, E., De Bruyne, E., Facon, T., Elewaut, D., Vanderkerken, K. & Menu, E. (2013b) Preclinical evaluation of invariant natural killer T cells in the 5T33 multiple myeloma model. *PLoS One*, **8**, e65075.

Quach, H., Ritchie, D., Stewart, A.K., Neeson, P., Harrison, S., Smyth, M.J. & Prince, H.M. (2010) Mechanism of action of immunomodulatory drugs (IMiDS) in multiple myeloma. *Leukemia*, **24**, 22–32.

Radl, J., De Glopper, E.D., Schuit, H.R. & Zurcher, C. (1979) Idiopathic paraproteinemia. II. Transplantation of the paraprotein-producing clone from old to young C57BL/KaLwRij mice. *Journal of Immunology*, **122**, 609–613.

Rajkumar, S.V., Leong, T., Roche, P.C., Fonseca, R., Dispenzieri, A., Lacy, M.Q., Lust, J.A., Witzig, T.E., Kyle, R.A., Gertz, M.A. & Greipp, P.R. (2000) Prognostic value of bone marrow angiogenesis in multiple myeloma. *Clinical Cancer Research*, **6**, 3111–3116.

Rawlings, J.S., Rosler, K.M. & Harrison, D.A. (2004) The JAK/STAT signaling pathway. *Journal of Cell Science*, **117**, 1281–1283.

Ria, R., Reale, A., De Luisi, A., Ferrucci, A., Moschetta, M. & Vacca, A. (2011) Bone marrow angiogenesis and progression in multiple myeloma. *American Journal of Blood Research*, **1**, 76–89.

Ribatti, D., Nico, B., Pezzolo, A., Vacca, A., Meazza, R., Cinti, R., Carlini, B., Parodi, F., Pistoia, V. & Corrias, M.V. (2006) Angiogenesis in a human neuroblastoma xenograft model: mechanisms and inhibition by tumour-derived interferon-gamma. *British Journal of Cancer*, **94**, 1845–1852.

Richter, J., Neparidze, N., Zhang, L., Nair, S., Monesmith, T., Sundaram, R., Miesowicz, F., Dhodapkar, K.M. & Dhodapkar, M.V. (2013) Clinical regressions and broad immune activation following combination therapy targeting human NKT cells in myeloma. *Blood*, **121**, 423–430.

Roccaro, A.M., Hideshima, T., Raje, N., Kumar, S., Ishitsuka, K., Yasui, H., Shiraishi, N., Ribatti, D., Nico, B., Vacca, A., Dammacco, F., Richardson, P.G. & Anderson, K.C. (2006) Bortezomib mediates antiangiogenesis in multiple myeloma via direct and indirect effects on endothelial cells. *Cancer Research*, **66**, 184–191.

Saha, B., Jyothi Prasanna, S., Chandrasekar, B. & Nandi, D. (2010) Gene modulation and immunoregulatory roles of interferon gamma. *Cytokine*, **50**, 1–14.

Schindler, C., Levy, D.E. & Decker, T. (2007) JAK-STAT signaling: from interferons to cytokines. *The Journal of Biological Chemistry*, **282**, 20059–20063.

Schroder, K., Hertzog, P.J., Ravasi, T. & Hume, D.A. (2004) Interferon-gamma: an overview of signals, mechanisms and functions. *Journal of Leukocyte Biology*, **75**, 163–189.

Sgadari, C., Angiolillo, A.L. & Tosato, G. (1996) Inhibition of angiogenesis by interleukin-12 is mediated by the interferon-inducible protein 10. *Blood*, **87**, 3877–3882.

Song, W., van der Vliet, H.J., Tai, Y.T., Prabhala, R., Wang, R., Podar, K., Catley, L., Shammas, M.A., Anderson, K.C., Balk, S.P., Exley, M.A. & Munshi, N.C. (2008) Generation of antitumor invariant natural killer T cell lines in multiple myeloma and promotion of their functions via lenalidomide: a strategy for immunotherapy. *Clinical Cancer Research*, **14**, 6955–6962.

Spanoudakis, E., Hu, M., Naresh, K., Terpos, E., Melo, V., Reid, A., Kotsianidis, I., Abdalla, S., Rahemtulla, A. & Karadimitris, A. (2009) Regulation of multiple myeloma survival and progression by CD1d. *Blood*, **113**, 2498–2507.

Strasly, M., Cavallo, F., Geuna, M., Mitola, S., Colombo, M.P., Forni, G. & Bussolino, F. (2001) IL-12 inhibition of endothelial cell functions and angiogenesis depends on lymphocyte-endothelial cell cross-talk. *Journal of Immunology*, **166**, 3890–3899.

Tandle, A., Blazer, D.G. 3rd & Libutti, S.K. (2004) Antiangiogenic gene therapy of cancer: recent developments. *Journal of Translational Medicine*, **2**, 22.

UKCCCR (1998) United Kingdom Co-ordinating Committee on Cancer Research (UKCCCR) Guidelines for the Welfare of Animals in Experimental Neoplasia (Second Edition). *British Journal of Cancer*, **77**, 1–10.

Vacca, A. & Ribatti, D. (2006) Bone marrow angiogenesis in multiple myeloma. *Leukemia*, **20**, 193–199.

Vacca, A., Ribatti, D., Roccaro, A.M., Frigeri, A. & Dammacco, F. (2001) Bone marrow angiogenesis in patients with active multiple myeloma. *Seminars in Oncology*, **28**, 543–550.

Van Kaer, L. (2005) alpha-Galactosylceramide therapy for autoimmune diseases: prospects and obstacles. *Nature Reviews Immunology*, **5**, 31–42.

Van Kaer, L. (2007) NKT cells: T lymphocytes with innate effector functions. *Current Opinion in Immunology*, **19**, 354–364.

Van Valckenborgh, E., De Raeve, H., Devy, L., Blacher, S., Munaut, C., Noel, A., Van Marck, E., Van Riet, I., Van Camp, B. & Vanderkerken, K. (2002) Murine 5T multiple myeloma cells induce angiogenesis in vitro and in vivo. *British Journal of Cancer*, **86**, 796–802.

Vanderkerken, K., Asosingh, K., Croucher, P. & Van Camp, B. (2003) Multiple myeloma biology: lessons from the 5TMM models. *Immunological Reviews*, **194**, 196–206.

Vanderkerken, K., Asosingh, K., Willems, A., De Raeve, H., Couck, P., Gorus, F., Croucher, P. & Van Camp, B. (2005) The 5T2MM murine model of multiple myeloma: maintenance and analysis. *Methods in Molecular Medicine*, **113**, 191–205.

Vivier, E., Ugolini, S., Blaise, D., Chabannon, C. & Brossay, L. (2012) Targeting natural killer cells and natural killer T cells in cancer. *Nature Reviews Immunology*, **12**, 239–252.

Voest, E.E., Kenyon, B.M., O'Reilly, M.S., Truitt, G., D'Amato, R.J. & Folkman, J. (1995) Inhibition of angiogenesis in vivo by interleukin 12. *Journal of the National Cancer Institute*, **87**, 581–586.

Yang, J. & Richmond, A. (2004) The angiostatic activity of interferon-inducible protein-10/CXCL10 in human melanoma depends on binding to CXCR3 but not to glycosaminoglycan. *Molecular Therapy*, **9**, 846–855.